Identification, molecular characterization, clinical prognosis, and therapeutic targeting of human bladder tumor-initiating cells

Keith Syson Chan[a,b,1], Inigo Espinosa[c], Mark Chao[a], David Wong[d], Laurie Ailles[a], Max Diehn[a], Harcharan Gill[b], Joseph Presti, Jr.[b], Howard Y. Chang[d], Matt van de Rijn[c], Linda Shortliffe[b], and Irving L. Weissman[a,1]

[a]Institute for Stem Cell Biology and Regenerative Medicine, Stanford Cancer Center, Stanford University School of Medicine, Stanford, CA 94304-5542; Departments of [b]Urology and [c]Pathology, Stanford University Medical Center, Stanford, CA 94305-5118; and [d]Program in Epithelial Biology, Stanford University, Stanford, CA 94305

Major clinical issues in bladder cancer include the identification of prediction markers and novel therapeutic targets for invasive bladder cancer. In the current study, we describe the isolation and characterization of a tumor-initiating cell (T-IC) subpopulation in primary human bladder cancer, based on the expression of markers similar to that of normal bladder basal cells (Lineage-CD44$^+$CK5$^+$CK20$^-$). The bladder T-IC subpopulation was defined functionally by its enriched ability to induce xenograft tumors in vivo that recapitulated the heterogeneity of the original tumor. Further, molecular analysis of more than 300 bladder cancer specimens revealed heterogeneity among activated oncogenic pathways in T-IC (e.g., 80% Gli1, 45% Stat3, 10% Bmi-1, and 5% β-catenin). Despite this molecular heterogeneity, we identified a unique bladder T-IC gene signature by gene chip analysis. This T-IC gene signature, which effectively distinguishes muscle-invasive bladder cancer with worse clinical prognosis from non-muscle-invasive (superficial) cancer, has significant clinical value. It also can predict the progression of a subset of recurring non-muscle-invasive cancers. Finally, we found that CD47, a protein that provides an inhibitory signal for macrophage phagocytosis, is highly expressed in bladder T-ICs compared with the rest of the tumor. Blockade of CD47 by a mAb resulted in macrophage engulfment of bladder cancer cells in vitro. In summary, we have identified a T-IC subpopulation with potential prognostic and therapeutic value for invasive bladder cancer.

antibody therapy | bladder cancer | cancer stem cell | CD44 | CD47

Epithelial tumors contain a heterogeneous population of cells (1), and this cellular heterogeneity can be characterized by differences in the histopathology and functional properties (e.g., anchorage-independent growth, proliferative capacities, and apoptotic responses to therapies) (2, 3). Some suggest that such intratumoral heterogeneity arises from genetic and epigenetic differences of tumor cells through selective pressure during tumor evolution. Recently emerging evidence supports the existence of a cellular hierarchy within epithelial tumors. At the top of this hierarchy is a tumor-initiating cell (T-IC) or cancer stem cell (CSC) population that can self-renew and differentiate to progeny cells, thus resulting in the observed cellular and functional heterogeneity of epithelial tumors (4, 5). Candidate T-ICs have been isolated in a variety of solid tumors, including breast (6, 7), brain (8), colorectal (9–11), head and neck (12), pancreatic (13), prostate (14), and melanoma (15), based primarily on the expression of CD44, CD133, ALDH, and ABCB5. However, controversy continues regarding the frequency and even the existence of T-ICs/CSCs. In transgenic mouse models of lymphoma and leukemia, it has been reported that more than 10% of tumor cells are tumor-initiating, suggesting that T-IC are not rare (16). Recently, Quintana et al. reported that in some circumstances a single human melanoma cell can form a melanoma xenograft when transplanted with Matrigel (BD Biosciences) into the skin of immunocompromised mice that lack T, B, and natural killer (NK) cells (17). Although no marker was able to identify a tumor-initiating subpopulation in that study, only 25% of single cells were able to form tumors (17). Nevertheless, these data did not disprove the existence of a tumor-initiating subpopulation. It is possible that more aggressive tumors such as melanoma and serially passaged xenografted tumors may contain higher fractions of T-ICs. Clinically, the relevance of T-ICs/CSCs has become more evident. These cells were shown to be more resistant to conventional therapies such as radiation (18, 19) and chemotherapy (20), underscoring the need to pursue the isolation, characterization, and eventual targeting of T-ICs from other cancers.

Bladder cancer is the second most common urological malignancy (21, 22) and probably originates from the transitional epithelium that is composed of 3 to 6 layers of basal, intermediate, and multinucleate umbrella cells (21, 23). There are 2 major subtypes of bladder cancer: non-muscle-invasive cancer, which frequently recurs but often has good prognosis, and muscle-invasive cancers with poor prognosis (21, 22). Approximately 15% of non-muscle-invasive cancers progress to invasive bladder cancer, but no prognostic markers are used in clinically for predicting this progression (21). Invasive bladder cancer is mostly incurable (>90%) when there is local or distal metastasis, but 10% of patients who had metastatic bladder cancer showed response to systemic chemotherapy following cystectomy. Although not completely reliable, tumor grade and stage, treatment, and the patient's history of tumor recurrence can influence the outcome of bladder cancer. The objective of the current study is to provide an initial phenotypic and molecular characterization of bladder T-ICs and to examine their clinical relevance.

Results

Establishment of a Xenograft Model for Human Bladder Cancer. To examine whether a tumor-initiating subpopulation exists in bladder cancers, we first established a reliable in vivo xenograft model for human bladder cancer cells. Cells isolated from primary bladder cancer samples were mixed with Matrigel (BD Biosciences) and injected intradermally into mice deficient in the recombinase-activating gene 2 (*RAG2*) and the common cytokine receptor γ chain (γc) (*RAG2$^-$/γc$^-$ mice*) (24). These mice lack T, B, and NK cells and have been shown to be more efficient in human primary cell engraftment than nonobese diabetic/SCID mice (24). Specifi-

Table 1. Comparison of the number of tumorigenic cells among distinct tumor subpopulations in bladder cancer.

Cell number engrafted		100	500	1000–3000	5000	1×10^4	$2–3 \times 10^4$	5×10^4	1×10^5	$2–2.5 \times 10^5$	$3–5 \times 10^5$
Patient tumors	CD44$^+$	—	—	2/4	—	2/4	1/6	—	2/2	1/1	—
	CD44$^-$	—	—	0/4	—	0/4	0/6	—	0/2	0/3	2/2
Specimen no.				BC-8/11/12		BC-6/8	BC- 6/11/12		BC-8	BC-1	BC1/8
Xenograft tumors	CD44$^+$	1/4	1/2	2/4	8/9	—	4/4	9/9	5/5	—	—
	CD44$^-$	0/4	0/2	0/4	0/9	—	1/4	4/9	2/5	3/3	—

Immunocompromised mice ($RAG2^-/\gamma c^-$) were injected intradermally with tumor cell subpopulations (CD44$^+$/CD44$^-$) that were isolated by FACS with > 98% purity. Mice were monitored for at least 6 months before considered negative for engraftment. Cell number required for tumor formation is shown for bladder cancers (BC-1, -6, -8, -11, and -12). BC-1 and BC-8 were serially passaged into secondary and tertiary transplantation.

cally, cell suspensions of 14 freshly isolated bladder cancer specimens (BC-1 to BC-14) were injected after fractionation by flow cytometry before injection. Of the 14 tumors, 5 (35.7%) successfully engrafted [supporting information (SI) Table S1], usually with latency of 3 months. We found that the engraftment ability of bladder cancers was associated with the tumor invasion, degree of spread to lymph nodes, and distal metastasis (TNM staging) of original patient specimens; that is, the more invasive the primary tumor, the more likely was the tumor to be engrafted (Table S1). Histopathological analysis revealed that xenografted tumors (Fig. S1 B, D, and F) retained histology resembling that of the original patient tumor (Fig. S1 A and C).

Heterogeneity in the Immunophenotype of Human Bladder Cancer. To identify a putative T-IC subpopulation, cell suspensions of human bladder cancers were analyzed with a panel of stem cell markers including CD44, CD133, CD49f/integrinα6, CD166, CD105, and c-kit, and markers that define epithelial differentiation (e.g., CD24 and epithelial specific antigen). Blood and endothelial cells were excluded based on the expression of CD45 and CD31, respectively. Through screening with these markers, we found considerable heterogeneity in the immunophenotype across tumor specimens (Fig. S2). CD44 was expressed in 13 of 14 bladder tumors analyzed, comprising ≈3% to 36.3% of the total population (Table S1). We fractionated CD44$^+$ and CD44$^-$ cells by FACS (Becton Dickinson) and injected them into $RAG2^-/\gamma c^-$ mice. In 5 advanced-stage bladder cancers, the CD44$^+$ tumor cell subpopulation was consistently 10- to 200-fold enriched for T-ICs, as revealed by their enhanced ability to form xenografts in $RAG2^-/\gamma c^-$ mice as compared with CD44$^-$ cells from the same tumor (Table 1; Fig. S3). As few as 100 to 1,000 CD44$^+$ tumor cells were able to form xenografts in vivo (Table 1), whereas at least 2.0 to 5.0×10^4 CD44$^-$ tumor cells were necessary to induce xenografts (Table 1).

Bladder Cancer Tumor-Initiating Cells Express Markers Shared with Normal Bladder Basal Cells. In normal bladder urothelium, CD44 is expressed primarily in the basal cells (Fig. S4A). It has been proposed that normal basal cells that express cytokertain 5 (CK5$^+$) (Fig. S4B) can differentiate into intermediate and CK20$^+$ umbrella cells. It is reasonable to propose that the CD44$^+$ tumor cells also may give rise to CD44$^+$ and CD44$^-$ progeny, as do normal urothelial basal cells. Indeed, data from our study revealed that pure CD44$^+$ tumor cells could give rise to tumors containing both CD44$^+$ cells (black box in Fig. 1A) and CD44$^-$ cells (red box in Fig. 1A) as analyzed by flow cytometry (BC-1 and BC-8). The histology of xenografts formed from CD44$^+$ tumor cells shows areas of less differentiated (asterisks in Fig. S5A) and terminally differentiated cells (arrowheads in Fig. S5A). Immunofluorescence analysis of these xenografts revealed that many CD44$^+$ tumor cells (Fig. 1B, red) co-express CK5 (Fig. 1B, green), and CD44- tumor cells often co-express CK20 (Fig. 1C, green) (Table S2). Further, CD44$^+$ tumor cells (BC-1 and BC-8) were able to form tumors that could be serially transplanted for at least 3 additional passages. In these passages, CD44$^+$ tumor cells persisted as the T-ICs (Table 1). In

contrast, high numbers of CD44$^-$ tumor cells (BC-8) were unable to generate secondary tumors upon serial transplantation, and xenografts formed from CD44$^-$ tumor cells remained primarily CD44$^-$, with histology revealing high keratinization and features of terminally differentiated cells (arrowheads in Fig. S5B).

Further, we examined the relative co-localization of CD44 with CK5 and CK20 in a tissue array containing more than 300 bladder cancer specimens by immunohistochemistry. The results were summarized in a colorimetric representation in Fig. 1D. Approximately 40.4% of the tissue sections stained positive for CD44 (red), and 59.6% stained negative for CD44 (green). Multivariate regression analysis revealed a statistically significant correlation of CD44 with CK5 expression ($P < 0.0001$) but not with CK20 expression ($P = 0.8160$) (Fig. 1D). In bladder cancers expressing all 3 markers (i.e., CD44, CK5, and CK20) (arrow in Fig. 1D), the CD44$^+$ tumor
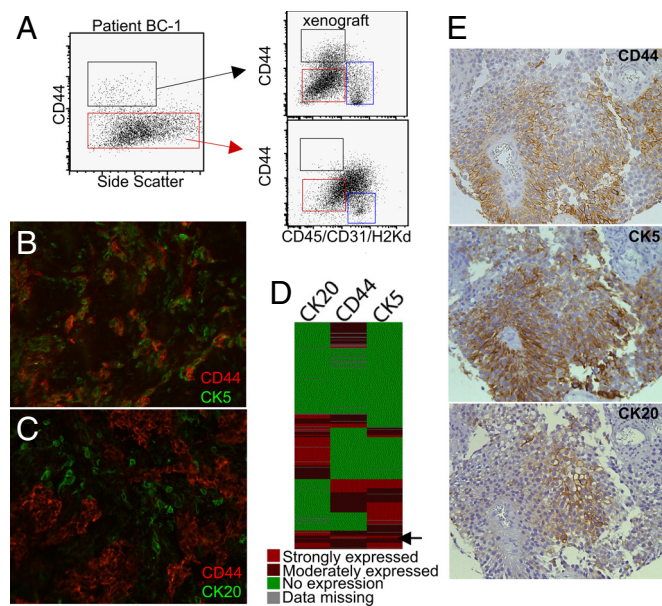

Fig. 1. Bladder tumor-initiating cells possess cell properties in common with bladder basal cells. (A) FACS (Becton Dickinson) analysis of CD44 expression in BC-1 and serially derived xenograft tumors. Infiltrating mouse cells positive for CD45 (hematopoietic cell marker), CD31 (endothelial cell marker), and H2Kd (mouse MHC class I) are indicated in blue boxes. Patient CD44$^+$ tumor cells (*black box*) can form xenografts comprised of both CD44$^+$ (*black box*) and CD44$^-$ (*red box*) tumor cells, whereas patient CD44$^-$ tumor cells form xenograft tumors comprised primarily of CD44$^-$ tumor cells (*red box*). (B and C) Immunofluorescence analysis of CD44 (*red*) and CK5/CK20 (*green*) in a representative bladder xenograft section. (D) Heatmap summarizing the relative expression of CD44, CK5, and CK20 by immunohistochemistry in bladder cancer tissue array containing ≈300 specimens. Arrow indicates a subgroup of bladder cancers expressing all 3 markers (CD44, CK5, and CK20). (E) Representative serial sections of bladder cancers showing the relative distribution of CD44, cytokeratin 5 (basal cell marker), and cytokeratin 20 (differentiated cell marker).
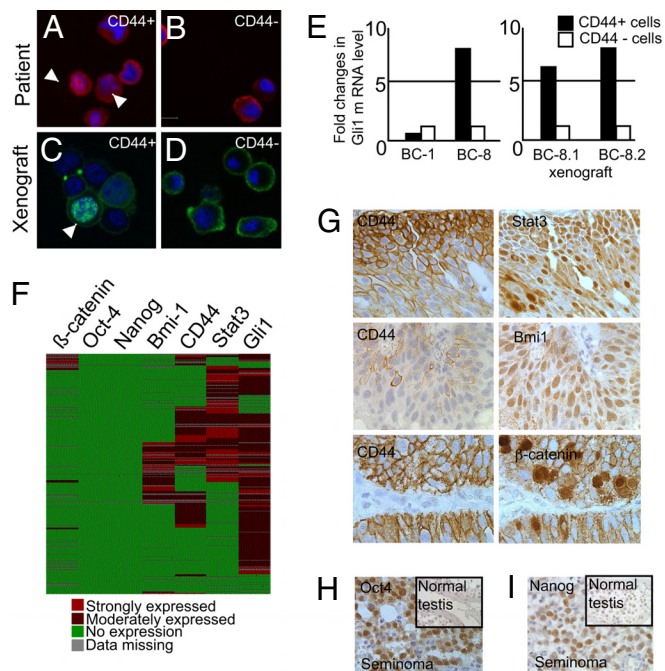
Fig. 2. Molecular heterogeneity: activation of diverse self-renewal proteins in bladder cancer. (*A–D*) Immunofluorescence staining of ß-catenin, followed by analysis with confocal microscopy. White arrowheads indicate cells with nuclear localization of ß-catenin. (*E*) Real-time PCR analysis of Gli1 mRNA level in fractionated tumor cells from BC-1, BC-8, and 2 representative xenografted tumors derived from BC-8. (*F*) Heatmap summarizing the expression level of CD44 and the activated forms of several self-renewal proteins. (*G*) Representative immunohistochemical staining of bladder cancers with positive CD44 expression and nuclear localization of β-catenin, Stat3, and Bmi-1 in serial sections. (*H* and *I*) Immunohistochemical staining of Oct-4 (*H*) and Nanog (*I*) in seminomas as positive control and staining in normal testis as negative control.

cells often co-localize with CK5 and are mutually exclusive to CK20 localization (Fig. 1*E*).

The cellular morphology of CD44$^+$ and CD44$^-$ tumor cells were analyzed in 4 freshly isolated tumors (BC-1, -3, -8, and -13). Purified cells were prepared by cytospinning followed by Giemsa-Wright staining. In 2 bladder cancers (BC-1 and -3), CD44$^+$ tumor cells possessed a high nuclear to cytoplasmic ratio; they were relatively smaller and were homogenous in size (Fig. S5*C*, BC-3). These characteristics are typical of normal basal cells. In contrast, CD44$^-$ tumor cells were more heterogeneous in size (of moderate size and larger), as is characteristic of differentiated cells (Fig. S5*C*, BC-3). In other cases (BC-8 and -13), there was no significant difference in the cellular morphology of CD44$^+$ and CD44$^-$ cells. Additional specimens will be required to determine whether there is a morphological difference between CD44$^+$ and CD44$^-$ bladder cancer cells.

Molecular Heterogeneity: Activation of Diverse Oncoproteins in Tumor-Initiating Cells Among Bladder Cancer Patients. To characterize bladder T-ICs at the molecular level, we examined the expression of several oncoproteins (4, 12, 25, 26) that have been implicated in the self-renewal of adult or embryonic stem cells (27–30). These oncoproteins include β-catenin, Bmi-1, Stat3, Gli1, Oct-4, and Nanog. In bladder cancer BC-1, we found the nuclear, activated form of β-catenin in $\approx$ 30% of the CD44$^+$ tumor cells (Fig. 2 *A* and *C*), whereas we found the membranous/cytoplasmic inactive form of β-catenin in 100% of the CD44$^-$ tumor cells (Fig. 2 *B* and *D*). In the next specimen, BC-8, we did not observe nuclear localization of β-catenin, but the mRNA level of Gli1 was highly expressed in CD44$^+$ T-ICs in comparison with CD44$^-$ tumor cells (Fig. 2*E*).

These data suggested that CD44$^+$ T-ICs from different patients may activate distinct self-renewal pathways.

To address this hypothesis in a large set of patient specimens, we analyzed the relationship of CD44 expression with additional oncoproteins in a bladder cancer tissue microarray. Immunohistochemical analysis or in situ hybridization revealed a heterogeneous profile in the active states of β-catenin, Gli1, Stat3, Bmi-1, Oct-4, and Nanog in bladder cancer. The expression profile is summarized in Fig. 2*F*. Specifically, the nuclear active form of β-catenin was found in 5% of bladder cancers, the nuclear localization of Bmi-1 was observed in 20% of bladder cancers, the nuclear active form of Stat3 was found in 40% of bladder cancers, and more than 80% of bladder cancers express Gli1 mRNA as detected by in situ hybridization (Fig. 2*F*). None of the bladder cancer specimens was found to express either Oct-4 or Nanog in the cytoplasm or nucleus (Fig. 2*F*). Detailed analysis revealed that although a large fraction of nuclear Stat3- (Fig. 2*G*) or Bmi-1-positive cells (Fig. 2*G*) co-localized with CD44$^+$ tumor cells, their expression was not completely restricted to CD44$^+$ tumor cells. In the bladder cancer specimens that exhibited nuclear β-catenin, it was expressed more restrictedly in the CD44$^+$ tumor cell subpopulation (Fig. 2*G*).

Bladder Tumor-Initiating Cell Gene Signature Predicts the Progression of a Subset of Non-Muscle-Invasive into Muscle-Invasive Bladder Cancer. Fifteen percent of non-muscle-invasive bladder cancers progress to the muscle-invasive disease (Fig. 3*A*). Reliable prognostic markers for predicting this progression are yet to be estab-
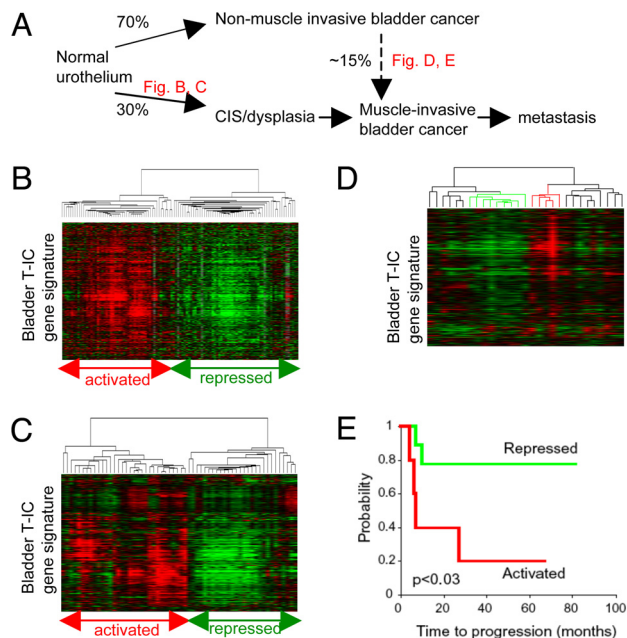

Fig. 3. Bladder T-IC gene signature predicts the progression of non-muscle-invasive to muscle-invasive bladder cancers. (*A*) Schematic diagram depicting the clinical progression of the 2 major subtypes of bladder cancers. Thirty percent of cases begin as carcinoma in situ/dysplasia that progresses to muscle-invasive bladder caner. Seventy percent of bladder cancers are non-muscle-invasive, and 15% of these can progress to invasive cancer. (*B* and *C*) Unsupervised hierarchical clustering of bladder T-IC signature genes from bladder cancer specimens obtained from 2 separate sets of published microarray data. Red indicates an activated bladder T-IC gene signature, and green indicates a repressed bladder T-IC gene signature. Approximately 97% (*B*) and 87% (*C*) of non-muscle-invasive bladder cancer clustered into the subgroup with the repressed bladder T-IC gene signature. (*D*) Unsupervised hierarchical clustering of bladder T-IC signature genes from published gene-expression data of non-muscle-invasive bladder cancer samples with long-term clinical follow-up. (*E*) Kaplan-Meier analysis of disease progression in patients who had bladder cancer categorized by an activated (*n* = 5) or repressed (*n* = 9) T-IC gene signature as shown in *D*.

Fig. 4. CD47 as a putative therapeutic target for eradicating bladder tumor-initiating cells. (*A*) Relative CD47 cell-surface protein expression on bulk bladder cancer cells in CD44$^+$ and CD44$^-$ subpopulations from human bladder cancer samples quantified by FACS (Becton-Dickinson). Mean fluorescence intensity was determined for each specimen. All samples except BC-8* were primary tumors human cells; BC-8* was sorted from a xenograft. (*B*) H&E staining of a xenografted bladder cancer (BC-6) at an early stage underneath the mouse skin of $RAG2^-/\gamma c^-$ mice. Islands of tumor cells (TC) grow around blood vessels (BV). (*C*) Immunofluorescence staining showing the relative distribution of CD44 (*red*) and CD47 (*green*) in xenografted tumor cells derived from BC-6; yellow color indicates co-localization of CD44 and CD47. (*D*) CFSE-labeled bladder cancer cells (from BC-1) were incubated with mouse bone marrow-derived macrophages in the presence of IgG1 isotype control, anti-HLA IgG1, or anti-CD47 IgG1 mAb. After 2 hours, the presence of fluorescently labeled bladder cancer cells within macrophages (*arrowheads*) was observed by immunofluorescence microscopy. (*E*) Phagocytosis of lineage-depleted human bladder cancer cells by mouse macrophages for each antibody condition per sample is shown. The phagocytic index for each antibody condition was determined by calculating the number of phagocytosed cells per 100 macrophages. Horizontal bars indicate the mean value for bladder cancer samples. (*F*) Phagocytosis of the same human bladder cancer samples by human macrophages for each antibody condition per sample is shown. Horizontal bars indicate the mean value for bladder cancer samples.
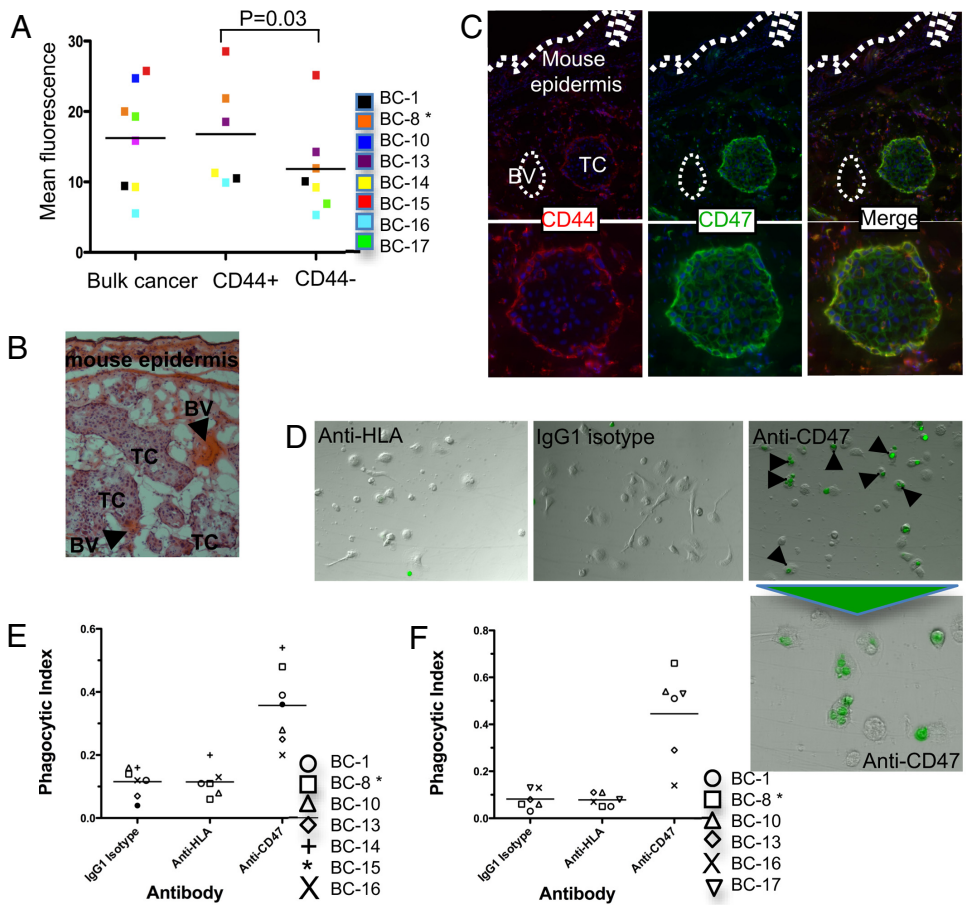
lished. We hypothesized that the alterations in gene expression within bladder T-IC will reveal important information about the pathogenesis of bladder cancers. Therefore, we used Affymetrix U133A GeneChip technology to examine the differences in the global gene-expression profiles of purified CD44$^+$ and CD44$^-$ tumor cells from 3 independent bladder cancers (BC-1, BC-8, and BC-14). Paired analysis using the Statistical Analysis of Microarrays (SAM) software (Stanford University, Stanford, CA) with a 5% false discovery rate identified a panel of 477 genes that are up-regulated in CD44$^+$ bladder T-ICs (referred to as the "bladder T-IC gene signature").

We first examined the similarity of this T-IC gene signature to the gene-expression profiles of bulk bladder cancer previously reported in the literature. In 2 distinct sets of published data containing 105 and 41 bladder cancers, respectively (31, 32), unsupervised hierarchical clustering of these data revealed 2 major subgroups: those with an activated bladder T-IC gene signature (*red*), and those with a repressed bladder T-IC gene signature (*green*) (Fig. 3 *B* and *C*). The majority of non-muscle-invasive bladder cancers from these 2 data sets exhibited a repressed bladder T-IC gene signature (97% and 87%, respectively) and can be distinguished from the muscle-invasive cancers, which exhibited an activated T-IC gene signature (Fig. 3 *B* and *C*). Unfortunately, no clinical outcome data were available to determine whether the subgroup of bladder cancer with an activated T-IC gene signature had a worse clinical outcome.

We further investigated the relevance of the bladder T-IC gene signature in the progression of non-muscle-invasive bladder cancers by analyzing the gene-expression profile of 29 non-muscle-invasive

bladder cancers with long-term survival follow-up (32). As indicated in Fig. 3 *B* and *C*, the majority of non-muscle-invasive cancers exhibited a repressed T-IC gene signature. Unsupervised hierarchical clustering differentiated these 29 expression profiles into 2 clear subgroups, activated (*n* = 5) and repressed (*n* = 8) (Fig. 3*D*). Kaplan-Meier analysis of the data from these 2 subgroups revealed a statistically significant difference in the time to progression for the patients in the 2 groups (*P* < 0.03) (Fig. 3*E*). Patients whose samples exhibited an activated T-IC gene signature did significantly worse, with a statistically significant shorter time to recurrence (25 months) (Fig. 3*E*, *red*). In contrast, ≈ 80% of the patients who had non-muscle-invasive bladder cancer with a repressed T-IC gene signature did not progress for as long as 80 months (Fig. 3*E*, *green*). These data clearly suggest that the bladder T-IC signature may be an important prognostic tool for predicting the progression of non-muscle-invasive bladder cancer to muscle-invasive bladder cancer.

CD47 Is Expressed on Bladder Cancer Tumor-Initiating Cells. Further, we analyzed cell-surface proteins that are expressed in our gene chip in attempt to identify therapeutic targets; one of these proteins was CD47. FACS (Becton Dickinson) analysis revealed a statistically significant higher protein expression of CD47 in CD44$^+$ T-ICs than in CD44$^-$ cells (*P* = 0.03) (Fig. 4*A*). Further, immunofluorescence analysis confirmed that CD47 is expressed in at least 80% of tumor cells (Fig. 4*C*, *green*), and CD44$^+$ cells (Fig. 4*C*, *red*) showed a high CD47 level compared with the CD44$^-$ population (Fig.). 4. Histologically, in the primary transplant nodules in

$Rag^-\gamma^-$ mice, the outer rim of cells in tumor nodules are $CD44^{hi}CD47^{hi}$, but most internal cells in the nodules are $CD44^-$ and $CD47^{low}$.

A Blocking Monoclonal Antibody Against CD47 Allows Phagocytosis of Human Bladder Cancer Cells in Vitro. CD47 is a ligand for the signal-regulatory protein alpha (SIRPα) expressed on phagocytic cells such as macrophages. The interaction of CD47 and SIRPα inhibits phagocytosis by macrophages (33). To examine whether disruption of the CD47−SIRPα interaction could stimulate phago-cytosis of bladder cancer cells, tumor cells were incubated in vitro with a blocking anti-CD47 mAb or with isotype-matched control mAbs in the presence of mouse or human macrophages. Incubation of tumor cells with mouse macrophages and anti-CD47 antibody enabled phagocytosis compared with the isotype control ($P = 0.03$) (Fig. 4 D and E). As negative controls, incubation of bulk bladder cancer cells with IgG1 isotype antibody or isotype-matched mouse anti-human HLA-A,B,C antibody did not result in significant phagocytosis ($P = 0.93$) (Fig. 4 D and E). To assess whether phagocytosis of human bladder cells by mouse macrophages in the presence of the anti-CD47 blocking antibody was the result of a xenogeneic recognition, we investigated the ability of human mac-rophages to phagocytose CD47-expressing human bladder cancer cells. Similarly, incubation of bladder cancer cells with human macrophages and anti-CD47 blocking antibody enabled phagocy-tosis as compared with isotype control antibody ($P = 0.01$) (Fig. 4F), whereas negative control IgG1 isotype antibody or mouse anti-human HLA-A,B,C antibody did not result in significant phagocytosis ($P = 0.93$) (Fig. 4F).

Discussion

It is believed that bladder cancer arises from the slow-cycling urothelium, which turns over every 6 to 12 months. In a 3D culturing condition in vitro, cell populations enriched for basal urothelial cells have been shown to give rise to a full-thickness urothelium com-prised of intermediate and umbrella cells. This observation suggests the existence of a cellular hierarchy within the urothelium. Here, we provide evidence for the existence of a T-IC−enriched subpopu-lation within bladder cancer that shares cytokeratins and cell-surface markers with urothelial basal cells.

In a subset of the freshly isolated bladder cancer specimens analyzed, we were able to identify a population of bladder T-ICs that can give rise to xenograft tumors that recapitulate the heter-ogeneity of the original tumors [$CD44^+CK5^+CK20^-$ (T-ICs) and $CD44^-CK5^-CK20^+$ tumor cells (differentiated progeny)]. Bladder T-ICs can be serially transplanted and form tumors for at least 3 passages, and $CD44^+CK5^+CK20^-$ tumor cells continued to be enriched for T-ICs. In contrast, the $CD44^-CK5^-CK20^+$ tumor cells do not form tumors upon serial transplantation, reflecting their limited renewing and/or proliferative capacities. Recently, Shmelkov et al. demonstrated that CD133, a colorectal T-IC marker (9, 10), was expressed ubiquitously in colorectal tumor cells and that $CD133^-$ cells were primarily stromal or infiltrating im-mune cells (34). Here, our FACS (Becton Dickinson) and trans-plantation data were supported by immunofluorescence staining, showing that $CD44^-$ cells contain tumor-derived cells and ruling out the possibility that the $CD44^-$ fraction contains only stromal or infiltrating immune cells. Immunohistochemical analysis of a large set of human bladder cancers revealed some tumors that are negative for CD44. This result reflects the heterogeneity of bladder cancer and indicates that CD44 is not a general marker for all bladder T-ICs. This finding is consistent with results found in other systems including breast cancer (35) and acute myeloid leukemia (AML).

The heterogeneity within bladder cancers is supported further by our data showing different activation states of oncoproteins also known to be involved in the self-renewal of stem cells. There is a strong link between the exposure to chemical carcinogens and the development of bladder cancer. Several decades ago, Prehn and Main showed that carcinogen-induced epithelial tumors expressed tumor antigens specific for each tumor and its many generations of daughter cells; each independent tumor only expressed its own tumor unique antigens (36). Our findings of heterogeneity of surface markers and self-renewing signal transduction pathways similarly suggest that there are multiple ways for epithelial cells to acquire oncogenic transformations.

Furthermore, our gene chip data comparing the T-IC–enriched population with non-T-IC cells revealed a signature comprised of genes that are elevated in bladder T-ICs. Importantly, this gene signature identified from only a small subset of patient specimens sheds light on major questions to be answered in the field of bladder cancer. Urological oncologists have been attempting to identify the subset of patients who have non-muscle-invasive bladder cancer whose disease will progress to incurable muscle-invasive cancer. Such prognostic information would lead to more aggressive treat-ments at an earlier time point to reduce the likelihood of the progression to advanced-stage cancer. The time to recurrence of non-muscle-invasive bladder cancer is significantly shorter in pa-tients who have an activated bladder T-IC signature than in those who have a repressed signature. Some of the genes within this gene signature, such as *Twist* (37) previously have been implicated in bladder cancer progression. Other cell-cycle–related proteins such as p21 and p27 have been implicated in recurrence of bladder cancer, but it has been established that these proteins are regulated at the translational level, and they were not found in our gene signature. Obviously, this signature must be validated using a larger number of samples before one can establish a link to clinical applications. Nevertheless, our data clearly implicate a biological involvement of bladder T-ICs and the genes unique to this sub-population in the "invasive-switch" of bladder cancer.

Finally, we attempted to identify therapeutic targets. Guided by the indications from our gene chip data, and other data obtained from in our laboratory, that CD47 plays a role in inhibiting macrophage phagocytosis of leukemia stem cells, we postulate that increased CD47 expression also may be a mechanism for bladder cancer pathogenesis. We previously have shown that human AML stem cells overexpress CD47 compared with resting hematopoietic stem cells and that antibody blockade of CD47 enables AML cells to be phagocytosed. Interestingly, CD47 is expressed in the majority of bladder cancer cells analyzed but is expressed at a higher level in the $CD44^+$ T-ICs, providing an attractive target for potential therapeutic intervention. Our initial studies demonstrated that CD47-expressing bladder cancer cells normally evade phagocytosis in vitro. Remarkably, disruption of the CD47–Sirpα interaction by anti-CD47 blocking antibody induced phagocytosis and subsequent elimination of bladder cancer cells in vitro. The isotype-matched anti-HLA antibody, which also binds bladder cancer cells (Fig. S6), failed to enhance phagocytosis, indicating that anti-CD47 antibody likely functions through the CD47–SIRPα mechanism and not through Fc receptor-mediated antibody opsonization. In addition, the anti-CD47 antibody is a mouse IgG1 isotype, which is less effective than IgG2 isotypes in engaging mouse Fc receptors (38). Future steps include investigating the in vivo effect of anti-CD47 antibody; it is interesting to speculate that CD47 mAbs may target bladder T-ICs and their downstream progenies for elimination in vivo.

In conclusion, we describe the identification of T-IC in bladder cancer, a T-IC gene signature that is associated with invasive characteristics and shorter time to progression and is a candidate therapeutic target. The T-IC population was found in a subset of the samples analyzed and reflected the molecular and cellular heter-ogeneity that is prevalent in bladder cancers. Further validation of this signature could lead to prognostic markers for predicting progression to invasive bladder cancer. Finally, the increased ex-pression of CD47 in bladder T-ICs may provide a target for future therapeutic intervention. Together these data reveal important

insights into bladder cancer pathogenesis and may lead to significant prognostic and therapeutic advances.

Experimental Procedures

Bladder Tumor Tissue Dissociation. The Stanford Institutional Review Board approved the enrollment of human subjects under protocol 1512. Tumor tissues were dissociated in proteolytic (Accumax, Innovative Cell Technologies, Inc.), collagenolytic (200U Type I and 20U Type IV collagenase) (Sigma-Aldrich C-0130, C-5138) and DNase enzymes at 37 °C for 2 to 6 hours.

Analysis and Cell Separation by FACS (Becton Dickinson). Tumor cell suspensions were stained with phycoerythrin (PE)-conjugated anti-CD44 (BD PharMingen 550989) antibody, and lineage mixture containing Cy7-PE -conjugated anti-CD45 (BD PharMingen 557748; 553077), biotin-conjugated anti-CD31 (eBioscience 13–0319-82; 553371), and H2Kd (BD PharMingen 553564) antibodies. Flow cytometry analysis and cell sorting was performed on a BD FACSAria (Becton Dickinson) cell-sorting system under 20 psi with a 100-μm nozzle.

Transplantation of Tumor Cell Suspensions into Immunocompromised Mice. Tumor cells were suspended in Matrigel matrix (Becton Dickinson 354248) mixed with media at a 1:1 ratio and were injected intradermally into the dorsal skin of $Rag2^-\gamma c^-$ mice at age of 4 to 8 weeks by 31-gauge insulin syringes (Becton Dickinson).

Immunohistochemical Staining and Data Analysis. Tumor cells were separated by FACS (Becton Dickinson) onto Plus slides fixed with 0.2% paraformaldehyde and then stained with anti-β-catenin antibody (Upstate 05–665 clone 8E7), followed by goat anti-mouse AlexaFluor 594/488 secondary antibodies (Molecular Probes). Paraffin-embedded tissue (10 μm) was deparaffinized and hydrated with graded ethanol. Antigen retrieval was performed with 1M EDTA at pH8.0 (for anti-β-catenin, BD Transduction Laboratories 610154) and 10 mM citrate buffer at pH6.0 [anti-CD44 (BD PharMingen 555477), anti-Oct-3/4 (Santa Cruz sc-5279), and anti-Bmi-1 (AbCam 14389–25)]. Staining was performed using the DAKO EnVision kit (K4006 and K4011) following the manufacturer's protocol. Tissue array data analysis and clustering was performed using a free online access program from Stanford Tissue Microarray Database (39), which is kindly supported by Robert J Marinelli.

In Vitro Phagocytosis Assay. Macrophages were plated at a density of 5×10^4 cells in a 24-well tissue-culture plate. Human bladder cancer cells were fluorescently labeled with carboxyfluorescein succinimidyl ester (CFSE) according to protocol (Invitrogen). After 2 hours, 2×10^4 CFSE-labeled bladder cancer cells were added to the macrophage-containing wells along with 7 μg/mL of IgG1 isotype (Ebiosciences), anti-HLA-A,B,C (Ebiosciences), or anti-CD47 antibody and incubated for 2 hours. The phagocytic index was calculated as the number of GFP-positive cells per 100 macrophages.

1. Heppner GH (1984) Tumor heterogeneity. *Cancer Res* 44:2259–2265.
2. Kirkels WJ, Pelgrim OE, Debruyne FM, Vooijs GP, Herman CJ (1982) Soft agar culture of human transitional cell carcinoma colonies from urine. *Am J Clin Pathol* 78:690–694.
3. Lipponen PK, Eskelinen MJ (1992) Cell proliferation of transitional cell bladder cancer determined by PCNA/cyclin immunostaining. A histopathological description. *Anticancer Res* 12:577–583.
4. Reya T, Morrison SJ, Clarke MF, Weissman IL (2001) Stem cells, cancer, and cancer stem cells. *Nature* 414:105–111.
5. Polyak K, Hahn WC (2006) Roots and stems: Stem cells in cancer. *Nat Med* 12:296–300.
6. Al-Hajj M, Wicha MS, Benito-Hernandez A, Morrison SJ, Clarke MF (2003) Prospective identification of tumorigenic breast cancer cells. *Proc Natl Acad Sci USA* 100:3983–3988.
7. Ginestier C, et al. (2007) ALDH1 is a marker of normal and malignant human mammary stem cells and a predictor of poor clinical outcome. *Cell Stem Cell* 1:555–567.
8. Singh SK, et al. (2004) Identification of human brain tumour initiating cells. *Nature* 432:396–401.
9. Ricci-Vitiani L, et al. (2007) Identification and expansion of human colon-cancer-initiating cells. *Nature* 445:111–115.
10. O'Brien CA, Pollett A, Gallinger S, Dick JE (2007) A human colon cancer cell capable of initiating tumour growth in immunodeficient mice. *Nature* 445:106–110.
11. Dalerba P, et al. (2007) Phenotypic characterization of human colorectal cancer stem cells. *Proc Natl Acad Sci USA* 104:10158–10163.
12. Prince ME, et al. (2007) Identification of a subpopulation of cells with cancer stem cell properties in head and neck squamous cell carcinoma. *Proc Natl Acad Sci USA* 104:973–978.
13. Li C, et al. (2007) Identification of pancreatic cancer stem cells. *Cancer Res* 67:1030–1037.
14. Patrawala L, et al. (2006) Highly purified CD44+ prostate cancer cells from xenograft human tumors are enriched in tumorigenic and metastatic progenitor cells. *Oncogene* 25:1696–1708.
15. Schatton T, et al. (2008) Identification of cells initiating human melanomas. *Nature* 451:345–349.
16. Kelly PN, Dakic A, Adams JM, Nutt SL, Strasser A (2007) Tumor growth need not be driven by rare cancer stem cells. *Science* 317:337.
17. Quintana E, et al. (2008) Efficient tumour formation by single human melanoma cells. *Nature* 456:593–598.
18. Bao S, et al. (2006) Glioma stem cells promote radioresistance by preferential activation of the DNA damage response. *Nature* 444:756–760.
19. Diehn M, et al. (2009) Association of reactive oxygen species levels and radioresistance in cancer stem cells. *Nature* 458:780–783.
20. Li X, et al. (2008) Intrinsic resistance of tumorigenic breast cancer cells to chemotherapy. *J Natl Cancer Inst* 100:672–679.
21. Dinney CP, et al. (2004) Focus on bladder cancer. *Cancer Cell* 6:111–116.
22. Wu XR (2005) Urothelial tumorigenesis: A tale of divergent pathways. *Nature Reviews Cancer* 5:713–725.
23. Borden LS, Jr., Clark PE, Hall MC (2004) Bladder cancer. *Current Opinion in Oncology* 16:257–262.
24. Goldman JP, et al. (1998) Enhanced human cell engraftment in mice deficient in RAG2 and the common cytokine receptor gamma chain. *Br J Haematol* 103:335–342.
25. Hochedlinger K, Yamada Y, Beard C, Jaenisch R (2005) Ectopic expression of Oct-4 blocks progenitor-cell differentiation and causes dysplasia in epithelial tissues. *Cell* 121:465–477.
26. Chan KS, et al. (2004) Disruption of Stat3 reveals a critical role in both the initiation and the promotion stages of epithelial carcinogenesis. *J Clin Invest* 114:720–728.
27. Reya T, et al. (2003) A role for Wnt signalling in self-renewal of haematopoietic stem cells. *Nature* 423:409–414.
28. Park IK, et al. (2003) Bmi-1 is required for maintenance of adult self-renewing haematopoietic stem cells. *Nature* 423:302–305.
29. Niwa H, Burdon T, Chambers I, Smith A (1998) Self-renewal of pluripotent embryonic stem cells is mediated via activation of STAT3. *Genes Dev* 12:2048–2060.
30. Chambers I, et al. (2003) Functional expression cloning of Nanog, a pluripotency sustaining factor in embryonic stem cells. *Cell* 113:643–655.
31. Sanchez-Carbayo M, Socci ND, Lozano J, Saint F, Cordon-Cardo C (2006) Defining molecular profiles of poor outcome in patients with invasive bladder cancer using oligonucleotide microarrays. *J Clin Oncol* 24:778–789.
32. Dyrskjot L, et al. (2004) Gene expression in the urinary bladder: A common carcinoma in situ gene expression signature exists disregarding histopathological classification. *Cancer Res* 64:4040–4048.
33. Barclay AN, Brown MH (2006) The SIRP family of receptors and immune regulation. *Nature Reviews Immunology* 6:457–464.
34. Shmelkov SV, et al. (2008) CD133 expression is not restricted to stem cells, and both CD133+ and CD133− metastatic colon cancer cells initiate tumors. *J Clin Invest* 118:2111–2120.
35. Honeth G, et al. (2008) The CD44+/CD24− phenotype is enriched in basal-like breast tumors. *Breast Cancer Research* 10:R53.
36. Prehn RT (1970) Analysis of antigenic heterogeneity within individual 3-methylcholanthrene-induced mouse sarcomas. *J Natl Cancer Inst* 45:1039–1045.
37. Fondrevelle ME, et al. (2009) The expression of Twist has an impact on survival in human bladder cancer and is influenced by the smoking status. *Urologic Oncology* 27:268–276.
38. Nimmerjahn F, Ravetch JV (2007) Antibodies, Fc receptors and cancer. *Curr Opin Immunol* 19:239–245.
39. Marinelli RJ, et al. (2008) The Stanford Tissue Microarray Database. *Nucleic Acids Res* 36:D871–877.

MEDICAL SCIENCES